COMBINED HEAT AND POWER GENERATION BY ENHANCED GEOTEHRMAL SYSTEMS: COMPARISON OF DIRECT AND INDIRECT CONCEPTS FOR WATER AND SUPERCRITICAL CO_2 AS HEAT CARRIERS

Christopher Schifflechner[1*], Fabian Dawo[1], Sebastian Eyerer[1], Christoph Wieland[1] and Hartmut Spliethoff [1,2]

[1] Institute for Energy Systems, Faculty of Mechanical Engineering, Technical University of Munich, Boltzmannstraße 15, 85748 Garching, Germany

[2] Bavarian Center for Applied Energy Research, Garching, Germany
Walther-Meißner-Str. 6, 85748 Garching, Germany

* Corresponding Author: c.schifflechner@tum.de

ABSTRACT

Enhanced Geothermal Systems (EGS) contain a tremendous technical potential without major regional restrictions. Over the last years, several studies proposed the application of supercritical CO_2 (sCO_2) as a heat carrier for the utilization of geothermal resources as a promising alternative to the usage of water. The existing studies focus only on sole power generation projects. However, the current development of the geothermal sector in Europe increasingly emphasizes the combined heat and power production. Consequently, the annual available heat flow for power generation might differ significantly due to the varying heat demand. Thus, an assessment of the potential different power plant types for EGS should consider the part load characteristic of the different concepts. This work compares a thermosiphon with direct utilization of sCO_2 for power generation and a pumped brine system with power generation by an Organic Rankine Cycle. The comparison is carried out for defined reservoir conditions of 180°C and 49 MPa. The power generation through an ORC with R245fa displays the highest amount of produced net power during one year. For the ORC with R245fa the annual amount of net electricity is 11 % higher than for the ORC with R1233zd(E) and 10 % higher than for the sCO_2 case. The net power of the sCO_2 plant displays a significantly higher sensitivity to changes of the heat demand in comparison to brine systems with ORCs. The comparison of the ORC with R1233zd(E) and the sCO_2 thermosiphon shows a varying advantageousness depending on the current heat demand.

Keywords: Enhanced Geothermal Systems (EGS), Supercritical CO_2 (sCO_2), Organic Rankine Cycle (ORC), Geothermal, Combined Heat and Power (CHP), CO_2 Plume Geothermal (CPG) Systems

1. INTRODUCTION

Geothermal energy can play a significant role within the necessary energy transition for facing global warming. While the utilization of hydrothermal resources is limited to certain geological regions, Enhanced Geothermal Systems (EGS) have a tremendous technical potential without major regional restrictions (Chamorro et al., 2014). A commonly discussed EGS concept is the utilization of the hot rocks by pumping water (brine) through the geothermal reservoir. The hot brine is used as a heat source for a binary cycle such as an Organic Rankine Cycle (ORC) (Zhang and Jiang, 2012).

In the last years, an increasing focus is laid on the utilization of EGS with supercritical CO_2 (sCO_2) instead of water due to its beneficial fluid characteristics. The main advantages of sCO_2 are the non-polar fluid nature of CO_2 (the low salt solubility decreases the probability of scaling and corrosion within the system) and the favorable fluid properties of CO_2, which might enable a higher rate of heat extraction than with water (Atrens et al., 2010). In contrast to power generation by binary cycles for brine EGS, the sCO_2 can be used directly within a turbine for power generation. In addition, sCO_2 is favorable for the operation as a thermosiphon, due to the strong buoyancy effect, which results in a high self-driven flow rate of the sCO_2 without the necessity of an additional pump or compressor (Atrens et al., 2010).

Several studies compare the power output of both potential heat carriers. Adams et al. (2014) investigate the performance of a sCO_2 thermosiphon. The results reveal that the sCO_2 case is highly favorable in comparison to a brine thermosiphon case for most geothermal gradients and reservoir depths. For example, for a geothermal gradient of 35°C km^{-1} and a depth of 4 km, the generated power by the sCO_2 is around 2.5 times higher than for the ORC scenario. Only for a depth of 5 km and a very high gradient of 50°C km^{-1}, the brine case achieves comparable power output than the sCO_2 thermosiphon. Therefore, it can be concluded that the thermosiphon operation of water is not favorable for most geological conditions, since due to different fluid characteristic the achievable brine flow rate is significantly lower than for a sCO_2 thermosiphon. Adams et al. (2015) compare the direct sCO_2 system with a pumped indirect brine case. For smaller depths than 3 km, the direct sCO_2 utilization by a thermosiphon is favorable than an ORC with R245fa as working fluid, which is driven by pumped brine, while for depth between 3 and 5 km, the ORC case reveals higher power outputs than the direct sCO_2 thermosiphon and comparable power outputs for the pumped direct sCO_2 case.

The existing studies focus only on the comparison of different concepts for power generation. However, as it can be seen exemplary within the analysis of the Heat Roadmap Europe for local heat supply by Möller et al. (2019), geothermal energy might play a major role within this transformation. Therefore, also the utilization of EGS might focus on CHP projects, as it can be observed currently for the majority of hydrothermal projects such as in Germany (Eyerer et al., 2017). Consequently, the annual available heat flow for power generation might differ significantly due to the varying heat demand. Thus, an assessment of the potential different heat carriers for EGS should consider the part load characteristic of the power plant layout. Based on the heat demand characteristic of an actual district heating network, this study investigates the amount of produced net electricity, comparing sCO_2 and water as heat carrier for the utilization of geothermal resources.

2. METHODOLOGY

2.1 Plant layout

Within this work, two different geothermal plant layouts are investigated for combined heat and power generation with sCO_2 and brine as heat carrier, respectively. While for the sCO_2 case a thermosiphon operation is evaluated, the brine case considers a pumped operation, due to the low power output of brine thermosiphons as shown by Adams et al. (2014). With this additional brine pump, the achievable flow rate increases significantly, but also a high auxiliary demand is caused.

The plant layouts are presented in Figure 1. This work proposes a plant layout for the sCO_2 CHP case with two parallel streams. In one stream, the sCO_2 directly enters the turbine, while the second stream is first utilized for providing heat for the district heating network before entering a second turbine. After the turbines, the two streams are mixed before entering an air cooled condenser and flowing down the injection wellbore. As an alternative, a parallel geothermal CHP concept with a subcritical one-staged ORC is investigated. Next to the common working fluid R245fa, R1233zd(E) is investigated as an alternative. Due to the high Global Warming Potential (GWP) of R245fa, the application of low-GWP fluids such as R1233zd(E) result in a significantly better environmental performance of the geothermal plant (Heberle et al., 2016). Eyerer et al. (2019b) investigated the replacement of R245fa with R1233zd(E) in an ORC. The experiments reveal a 9 % higher power output of R245fa in comparison to R1233zd(E). Table 1 summarizes the main fluid properties of CO_2 and the two investigated ORC working fluids.

Table 1: Fluid properties (Heberle et al., 2016; Rony et al., 2019)

Fluid	T_{crit}	P_{crit}	GWP	Safety class
CO_2	31.1°C	7.38 MPa	1	A1
R245fa	154.1°C	3.65 MPa	1050	B1
R1233zd(E)	165.6°C	3.57 MPa	6	A1

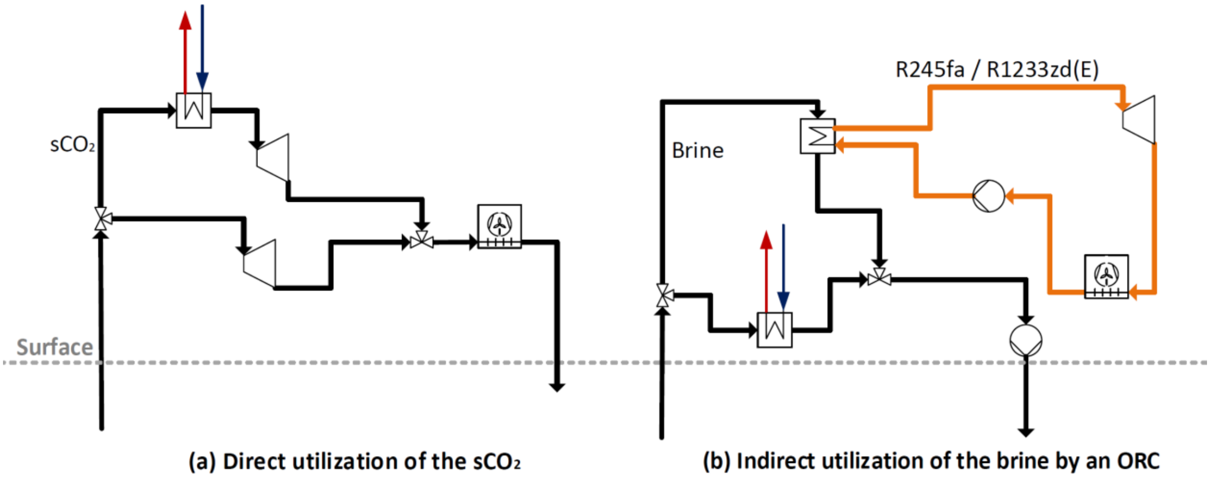

Figure 1: Plant layout for the (a) direct sCO_2 utilization and the (b) indirect utilization of the brine by a one-staged ORC

2.2 Heat demand profile

For analyzing the performance of the investigated CHP concepts, the operational data of a real district heating network are adapted. The general characteristic of the heat demand is taken from the open-source data of the district heating network by the Stadtwerke Flensburg GmbH (Kaldemeyer et al., 2019). The actual heat demand is scaled down to a maximal heat demand of 11 MW_{th}, which is a common demand size for geothermal CHP plants in Germany (Eyerer et al., 2017). The general characteristic of the annual load profile is similar to the one of a real German geothermal CHP plant, which is described by Dawo et al. (2019). The adapted heat demand and water flow rate of the district heating network are shown in Figure 2. The water of the district heating network enters and leaves the geothermal plant with an average temperature of 50°C and 95°C, respectively.

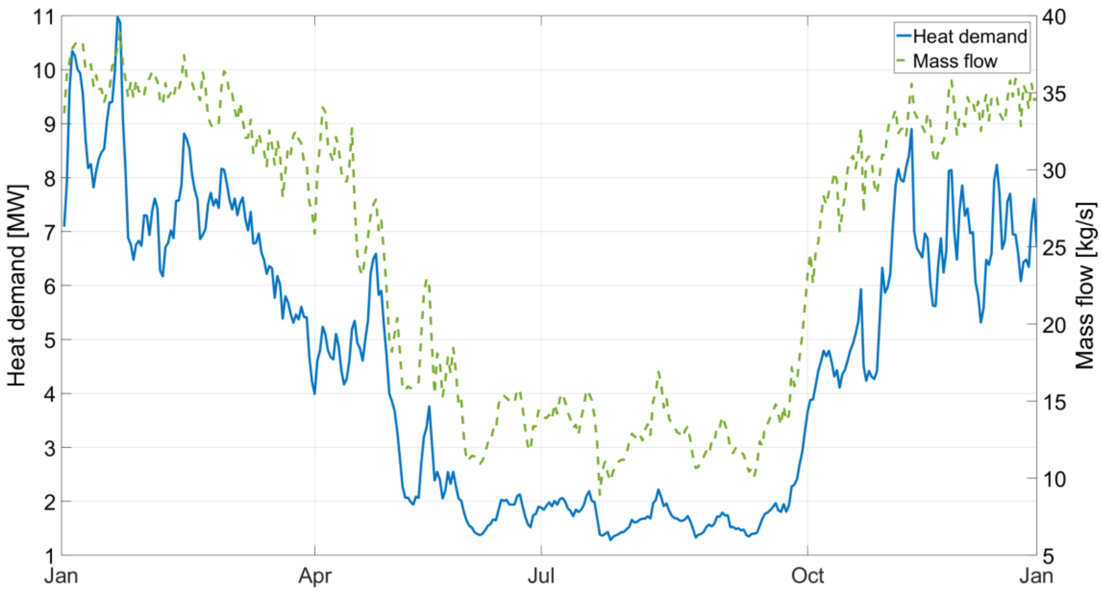

Figure 2: Characteristic of the district heating system (daily average)

2.3 Wellhead conditions

The results of Adams et al. (2015) show the high influence of the defined geological conditions and reservoir depths on the performance characteristic of different utilization concepts. Within this work, reservoir conditions which might be expected for an EGS system in Germany are applied. Therefore, a geothermal gradient of 34°C km^{-1} and a depth of 5 km is assumed. This results in reservoir conditions of 180°C and 49 MPa. Furthermore, a well pipe roughness ε of 55 μm and a pipe diameter D of 0.41 m are applied analogous to Adams et al. (2015). For comparing the performance of water and sCO_2 as heat carrier, the selection of the pipe diameter might have a strong impact. Thus, both concepts might have different optimal pipe diameter. However, in order to remain consistent with the most relevant publications (Adams et al., 2015; Adams et al., 2019; Hansper et al., 2019) and to ensure comparability with their results, the same diameter is assumed for both heat carriers. Especially the recent work by Hansper et al. (2019), which compares the thermodynamic performance of both heat carriers for sole power generation, applies also the assumption of an identical pipe diameter for both concepts. Thus, the following calculations are based on a pipe diameter of 0.41 m for both heat carriers.

The wellhead conditions are calculated by the subsequent formulas, which are described in detail by Atrens et al. (2010). Starting at the bottom of the production well, the change of the fluid properties is calculated iterative with length intervals of Δz = 50 m. The calculations are based on the assumptions of no heat flow across the boundaries of the wellbore and steady-state operation. All fluid properties are calculated using the REFPROP 9.1 database (Lemmon et al., 2013).

$$\Delta P = \rho g \Delta z \; - \; \Delta P_{f,well} \tag{1}$$

$$\Delta P_{f,well} = f \, \frac{\Delta z \, \rho}{D} \frac{V^2}{2} = f \, \frac{8 \, \dot{m}^2 \Delta z}{\pi^2 \rho D^5} \tag{2}$$

$$f = \left\{ -1.8 \log \left[\frac{6.9}{Re} + \left(\frac{\varepsilon}{3.7 \, D} \right)^{1.11} \right] \right\}^{-2} \tag{3}$$

$$\Delta h = g \Delta z - \frac{\Delta(V^2)}{2} \tag{4}$$

$\Delta P_{f,well}$ represents the pressure drop within one segment due to friction, f is the Darcy friction factor, Δh is the change of the fluid enthalpy and V the fluid velocity. Based on the previous equations and the defined reservoir pressure P_{Res}, the pressure at the wellhead P_{WH} is calculated.

$$P_{WH} = P_{Res} - \rho g \Delta z \; - \; \Delta P_{f,well} \tag{5}$$

Despite the same entry conditions for the production well, both fluids reveal significantly different wellhead conditions due to their strongly deviating fluid properties. Since the brine has liquid-like fluid properties, the enthalpy decrease affects mainly only the pressure, while the enthalpy decrease of the gas-like sCO_2 properties causes strong changes in temperature, volume and pressure (Atrens et al., 2010). Whereas the brine temperature decreases only by 7°C, the sCO_2 temperature at the wellhead is 57°C lower than the reservoir temperature. However, since the enthalpy decrease of the sCO_2 affects mainly the temperature, the pressure drop for sCO_2 is lower than for the brine.

Table 2 presents a summary of the model parameter and assumptions for the simulations. The injection conditions are adapted from Atrens et al. (2009). For the sCO_2 case, injection conditions are 64 MPa and 25°C. For the brine, a necessary injection pressure of 7 MPa is set, while the injection temperature is variable. A mass flow rate of 225 kg/s is chosen for both heat carries, based on the presented results in Atrens et al. (2010). The turbine and pump efficiencies are taken from Adams et al. (2015). The electricity demand of the fans for the air cooling is 0.15 kW per kg s^{-1} of air (Schlagermann, 2014).

Table 2: Summary of the model parameters and assumptions for the simulations

Parameter	Brine	sCO_2
Depth	5000 m	
Well diameter	0.41 m	
Well roughness	55 µm	
T_{Res}	180°C	
p_{Res}	49 MPa	
T_{WH}	173°C	123°C
P_{WH}	3 MPa	20.5 MPa
T_{Inj}	variable	25°C
p_{Inj}	7 MPa	64 MPa
Mass flow rate	225 kg/s	
Isentropic turbine eff.	0.8	0.78
Pump efficiency	0.8	-
Electricity demand of the fans	0.15 kW per kg s^{-1} of air flow	

3. RESULTS AND DISCUSSION

For the sCO_2 case as well as both ORC working fluids, the annual produced electricity is calculated. The main results are listed in Table 3. The application of the pumped brine with R245fa as working fluid for the ORC provides the highest amount of produced net electricity. The net output is 11 % higher than for an ORC with R1233zd(E) and 10 % higher than for the direct utilization of the sCO_2 thermosiphon. The choice between the brine and sCO_2 utilization results also in a significant difference between the ratio of the net and gross electricity produced by both concepts. While the difference is only 1.2 GWh_{el} for the sCO_2 case, it is up to 22.9 GWh_{el} for the case of an ORC with R245fa as working fluid. In addition, a scenario for sole power generation without an additional heat demand by a district heating network is computed for all three concepts. The analysis of this case reveals a significant change in the performance comparison of the direct sCO_2 and the indirect brine concept. For pure generation, the direct sCO2 utilization produces nearly the same amount of net electricity as the ORC with R245fa. While the missing heat demand increases the ORC performance only by 3 %, the direct sCO2 performance improves by 13 %. Thus, it can be concluded that an increasing heat demand has a significantly higher effect on the performance of the proposed sCO_2 concept than on brine driven ORCs.

Table 3: Annual produced electricity

	Combined Heat and power generation		Sole power generation	
Concept	**Net electricity**	**Gross electricity**	**Net electricity**	**Gross electricity**
Direct sCO_2	58.5 GWh_{el}	59.7 GWh_{el}	66.1 GWh_{el}	68.6 GWh_{el}
Indirect brine (R245fa)	65.1 GWh_{el}	88.0 GWh_{el}	67.0 GWh_{el}	90.3 GWh_{el}
Indirect brine (R1233zd(E))	58.1 GWh_{el}	77.8 GWh_{el}	59.8 GWh_{el}	80.9 GWh_{el}

Figure 3 shows the change of the daily average net power of the three investigated cases over one year. The results reveal that the net power of the R245fa case is the highest value for every day. Comparing the sCO_2 utilization and the ORC with R1233zd(E) reveals a change of the better part load performance depending on the heat demand. During the winter period with high heat demand, the ORC with R1233zd(E) has a up to 0.3 MW_{el} better performance than the sCO_2 plant. On the contrast, the sCO_2 plant shows up to 0.5 MW_{el} higher net power during the summer with low heat demand. Figure 3 also highlights the high impact of the heat demand on the performance of the sCO_2 plant. While both ORC plants have an annual variation of around 0.3 MW_{el}, the sCO_2 plant net power varies by 0.9 MW_{el} within the year.

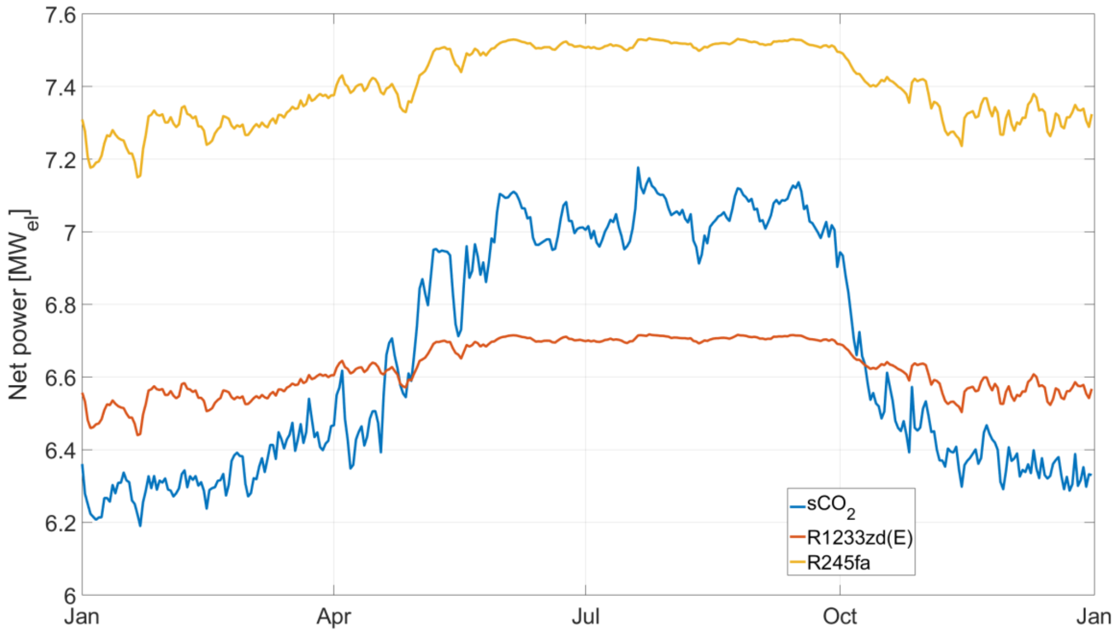

Figure 3: Daily average net power during one year

Figure 4 represents the composition of the electrical gross power for high heating demand during winter days and low heating demand during summer days. The analysis of the sCO_2 plant reveals the beneficial impact of the heat decoupling on the required fan power for cooling purposes. Since the high heat demand causes a strong decrease of the outlet temperature of the sCO_2 within the upper pipe flow (see Figure 1), the temperature of the mixed sCO_2 is significantly lower than during periods with low heat demand. Therefore, lower airflow rates are necessary for cooling. This effect compensates parts of the power reduction at the turbines.

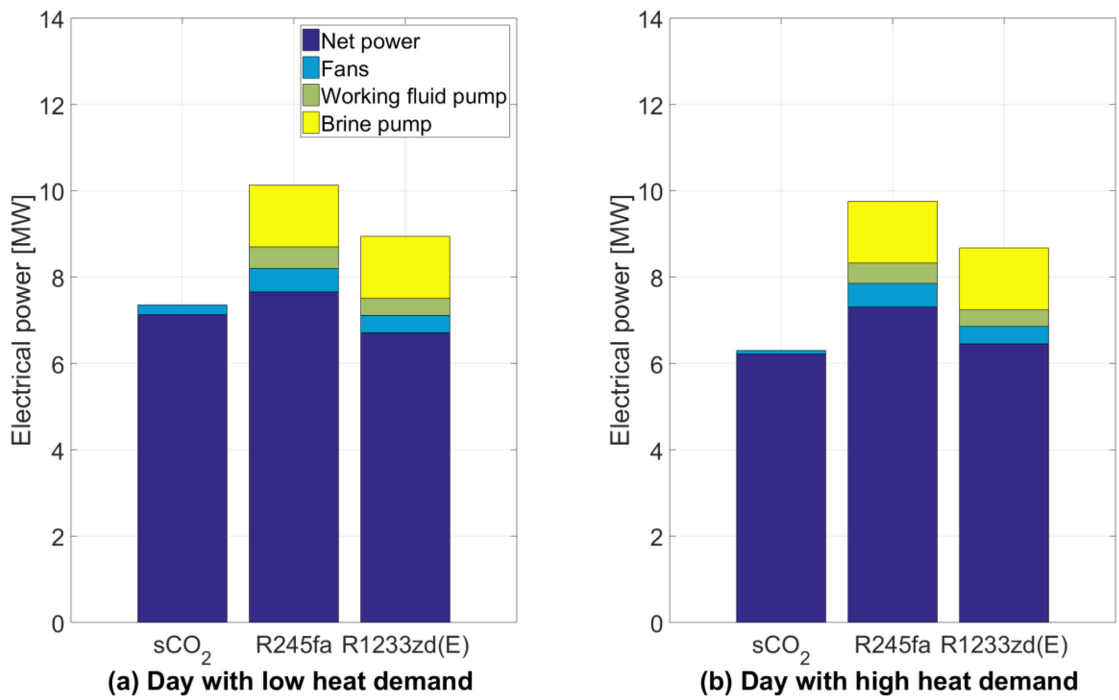

Figure 4: Results for selected days with (a) low heating demand and (b) high heating demand

4. CONCLUSION AND OUTLOOK

In this paper, the CHP performance of EGS with water and sCO_2 as heat carrier are evaluated for assumed reservoir conditions of 180°C and 49 MPa. The summarized key findings are:

- The power generation through an ORC with R245fa displays the highest amount of produced net power during one year. For the ORC with R245fa the annual amount of net electricity is 11 % higher than for the ORC with R1233zd(E) and 10 % higher than for the sCO_2 case.
- The produced amount of gross electricity by the R245fa ORC is 32 % higher than for the sCO_2 case. The auxiliary demand of the sCO_2 thermosiphon (2.3 %) is significantly lower than for the pumped ORC plant (33.0 %).
- The net power of the sCO_2 plant displays a significantly stronger sensitivity to changes of the heat demand in comparison to brine systems with ORCs. In case of sole power generation, the sCO_2 reveals a similar net power output as the brine system with an ORC with R245fa.
- During winter days the net power of sCO_2 is 5 % lower than for the R1233zd(E) ORC, whereas during periods with low heating demand the net power is 7 % higher.

Based on the results of the first detailed analysis of sCO_2 and water as heat carrier for EGS with CHP generation, more detailed evaluations should be carried out. This applies mainly to a broad range of geothermal gradients and reservoir depths. In addition, a detailed analysis of the impact of the district heating network's characteristic may be executed. Especially due to the strong cooling of the sCO_2 during the heat decoupling, the heat demand as well as the temperature profiles of the district heating might strongly influence the operation strategy of the sCO_2 plant. Furthermore, advanced plant layouts for sCO_2 projects may be developed and be compared to the performance of pumped brine systems with advanced plant layout strategies for ORC systems (cf. Eyerer et al. (2019a) and Wieland et al. (2016)).

NOMENCLATURE

CHP	Combined Heat and Power Generation	(–)
D	Well pipe inner diameter	(m)
EGS	Enhanced Geothermal Systems	(–)
f	Darcy friction factor	(–)
g	Acceleration due to gravity	(m s^{-2})
GWP	Global Warming Potential	(–)
$\dot{m}$	Mass flow rate	(kg s^{-1})
ORC	Organic Rankine Cycle	(–)
P	Pressure	(kPa)
Re	Reynolds number	(–)
sCO_2	supercritical CO_2	(–)
ε	Pipe surface roughness	(m)
ΔP	Pressure drop	(kPa)
Δz	Change of depth	(m)
ρ	Density	(kg m^{-3})

Subscript

crit	Critical
f,well	Friction within the borehole
Inj	Injection
WH	Wellhead

REFERENCES

References

Adams, B.M., Fleming, M.R., Bielicki, J.M., Hansper, J., Glos, S., Langer, M., Wechsung, M., Saar, M.O., 2019. Grid Scale Energy Storage using CO2 in Sedimentary Basins: The Costs of Power Flexibility. Proceedings of the European Geothermal Congress 2019.

Adams, B.M., Kuehn, T.H., Bielicki, J.M., Randolph, J.B., Saar, M.O., 2014. On the importance of the thermosiphon effect in CPG (CO2 plume geothermal) power systems. Energy 69, 409–418. 10.1016/j.energy.2014.03.032.

Adams, B.M., Kuehn, T.H., Bielicki, J.M., Randolph, J.B., Saar, M.O., 2015. A comparison of electric power output of CO2 Plume Geothermal (CPG) and brine geothermal systems for varying reservoir conditions. Applied Energy 140, 365–377. 10.1016/j.apenergy.2014.11.043.

Atrens, A.D., Gurgenci, H., Rudolph, V., 2009. CO 2 Thermosiphon for Competitive Geothermal Power Generation. Energy Fuels 23, 553–557. 10.1021/ef800601z.

Atrens, A.D., Gurgenci, H., Rudolph, V., 2010. Electricity generation using a carbon-dioxide thermosiphon. Geothermics 39, 161–169. 10.1016/j.geothermics.2010.03.001.

Chamorro, C.R., García-Cuesta, J.L., Mondéjar, M.E., Pérez-Madrazo, A., 2014. Enhanced geothermal systems in Europe: An estimation and comparison of the technical and sustainable potentials. Energy 65, 250–263. 10.1016/j.energy.2013.11.078.

Dawo, F., Wieland, C., Spliethoff, H., 2019. Kalina power plant part load modeling: Comparison of different approaches to model part load behavior and validation on real operating data. Energy 174, 625–637. 10.1016/j.energy.2019.02.173.

Eyerer, S., Dawo, F., Altnöder, M., Windhager, R., Niederdränk, A., Esch, H., Ausfelder, S., Konrad, R., Höger, M., Wieland, C., Spliethoff, H., 2019a. Design and first operation of an advanced ORC-CHP Architecture. 5th International Seminar on ORC Power Systems.

Eyerer, S., Dawo, F., Kaindl, J., Wieland, C., Spliethoff, H., 2019b. Experimental investigation of modern ORC working fluids R1224yd(Z) and R1233zd(E) as replacements for R245fa. Applied Energy 240, 946–963. 10.1016/j.apenergy.2019.02.086.

Eyerer, S., Hofbauer, S., Schifflechner, C., Wieland, C., Spliethoff, H., 2017. Potenzial der Geothermie im deutschen Energiesystem. BWK Das Energie-Fachmagazin 69, 62–65.

Hansper, J., Grotkamp, S., Glos, S., Langer, M., Wechsung, M., Adams, B.M., Saar, M.O., 2019. Assessment of Performance and Costs of CO2 Plume Geothermal (CPG) Systems. Proceedings of the European Geothermal Congress 2019.

Heberle, F., Schifflechner, C., Brüggemann, D., 2016. Life cycle assessment of Organic Rankine Cycles for geothermal power generation considering low-GWP working fluids. Geothermics 64, 392–400. 10.1016/j.geothermics.2016.06.010.

Kaldemeyer, C., Boysen, C., Tuschy, I., 2019. District heating network data for the city of Flensburg from 2014-2016. https://zenodo.org/record/2554082#.XMm3wPkzawU. Accessed 2 May 2019.

Lemmon, E.W., Huber, M.L., McLinden, M.O., 2013. NIST Standard Reference Database 23: Reference Fluid Thermodynamic and Transport Properties-REFPROP, Version 9.1, Standard Reference Data Program. National Institute of Standards and Technology: Gaithersburg, MD.

Möller, B., Wiechers, E., Persson, U., Grundahl, L., Lund, R.S., Mathiesen, B.V., 2019. Heat Roadmap Europe: Towards EU-Wide, local heat supply strategies. Energy. 10.1016/j.energy.2019.04.098.

Rony, R., Yang, H., Krishnan, S., Song, J., 2019. Recent Advances in Transcritical CO2 (R744) Heat Pump System: A Review. Energies 12, 457. 10.3390/en12030457.

Schlagermann, P., 2014. Exergoökonomische Analyse geothermischer Strombereitstellung am Beispiel des Oberrheingrabens. PhD Thesis, TU Munich.

Wieland, C., Meinel, D., Eyerer, S., Spliethoff, H., 2016. Innovative CHP concept for ORC and its benefit compared to conventional concepts. Applied Energy 183, 478–490. 10.1016/j.apenergy.2016.08.193.

Zhang, F.-Z., Jiang, P.-X., 2012. Thermodynamic analysis of a binary power cycle for different EGS geofluid temperatures. Applied Thermal Engineering 48, 476–485. 10.1016/j.applthermaleng.2012.04.028.

Zhu, J., Hu, K., Zhang, W., Lu, X., 2017. A study on generating a map for selection of optimum power generation cycles used for Enhanced Geothermal Systems. Energy 133, 502–512. 10.1016/j.energy.2017.05.130.

ACKNOWLEDGEMENT

Funding from the Bavarian State Ministry of Education, Science and the Arts in the framework of the project Geothermal-Alliance Bavaria is gratefully acknowledged.